

UV Diagnostics for the Energy Budget of Flares and CMEs

J. C. Raymond

Center for Astrophysics, 60 Garden St., Cambridge, MA 02176, USA.

e-mail: jraymond@cfa.harvard.edu

Abstract. Solar flares and coronal mass ejections convert large amounts of magnetic free energy into thermal, kinetic and potential energies, and into energy of non-thermal particles. The partitioning among these forms of energy is fundamental to both the physics of the eruptive events and the space weather consequences of the eruptions. This talk describes some aspects of the energy budget that can be derived from ultraviolet observations of the corona.

Key words. Sun: corona—flares—coronal mass ejections.

1. Introduction

The energy budget of solar flares and coronal mass ejections (CMEs) is the fundamental information needed to reach a physical understanding of the process. It is also the key information needed to apply our knowledge of solar activity to other astrophysical systems, ranging from solar-type stars to accretion disks around neutron stars and massive black holes.

It has proven very difficult to obtain a reliable energy budget for solar flare-CME events. No single wavelength band contains good diagnostics for all plasma conditions present, because gas from photospheric temperatures to tens of millions of Kelvins is present, and because non-thermal particles at very high energies contain a significant fraction of the energy. It is also very difficult to accurately measure the magnetic free energy. Finally, one must be careful not to double count components of the energy, as conversion of energy among magnetic, thermal, kinetic, radiative and non-thermal forms is the essence of the process.

The terms of the energy budgets have been compared in a few cases. Emslie *et al.* (2005) estimated the flare thermal and non-thermal energies and the CME kinetic and solar energetic particle (SEP) energies for two X-class events. They found that the magnetic, flare and CME energies were comparable, and that the flare energy in non-thermal particles was similar to that of the thermal plasma. Subramanian & Vourlidas (2007) measured the kinetic energies for several CMEs and estimated the magnetic energies from a magnetic flux rope model. They found comparable magnetic and kinetic energies. Akmal *et al.* (2001) and Ciaravella *et al.* (2001) compared the kinetic energies of CMEs with the heat that went into maintaining the plasma temperature in the face of adiabatic cooling, and they found that the two values were comparable.

Here we consider how ultraviolet spectroscopy can provide measurements of some of the terms in the energy budget. The ultraviolet wavelength range contains diagnostics for plasma as hot as 10 MK, and comparison of different spectral lines provides additional information about the line-of-sight component of velocity, the plasma composition, and through the ionization state, the thermal history of the plasma. Very few UV spectra of flares or of CMEs were available before the launch of SOHO, but now there are spectra covering a wide range of temperatures and velocities from CDS (e.g., Pike & Mason 2002), SUMER (e.g., Innes *et al.* 2001) and UVCS (see review by Kohl *et al.* 2006).

Here we discuss two applications of the UV spectroscopy to the energy budget problem; the radiative energy losses during the impulsive phase of an X-class flare, and the post-ejection heating of CME plasma as it travels away from the Sun.

2. Transition region emission in the impulsive phase of flares

During the impulsive phase of a solar flare, magnetic energy is transformed into several other forms, mainly the kinetic energy of non-thermal particles, heat of the flare plasma, electromagnetic radiation and kinetic energy of mass motions including coronal mass ejections and turbulence. Understanding the partitioning of energy among these forms is a necessary step to understand the physical processes involved. In large flares, the energy in non-thermal electrons inferred from the bremsstrahlung spectrum of hard X-rays is comparable to the thermal energy of the plasma that produces the $\sim 2 \times 10^7$ K soft X-ray emission (Holman *et al.* 2003; Emslie *et al.* 2005) and the kinetic energy of plasma ejected in the CME is comparable to those (Schwenn *et al.* 2006).

There are some difficulties in making this comparison, however. First, the thermal energy of the X-ray emitting gas is

$$E_{th} = \frac{3}{2}(n_e + n_p)kTV, \quad (1)$$

where n_e and n_p are the electron and proton densities, T is the temperature, and V is the volume. The temperature is measured from the soft X-ray spectrum, and the product $n_e n_p V$ is the emission measure, which can be derived from the luminosity and temperature. The difficulty is that there is seldom an accurate measure of the density or volume. It is sometimes assumed that V is the apparent volume estimated from X-ray images, but it is likely that the real volume is a small fraction of the apparent volume, given by a filling factor f (e.g., Aschwanden & Aschwanden 2006). If the filling factor is 0.1, the thermal energy estimated from the apparent volume is too large by a factor of 3.

The second difficulty is that a significant fraction of the thermal energy might be carried away from the X-ray emitting plasma by thermal conduction and radiated at lower temperatures. Estimates of the thermal conduction losses suffer from an uncertainty in filling factor, this time the areal filling factor of hot flux tubes at transition region temperatures, and from the possibility that classical thermal conduction as given by the Spitzer conductivity does not apply.

Ultraviolet spectra have the potential to address both of these questions, because there are density-sensitive line ratios in the UV and because most of the energy carried away by thermal conduction would be radiated away in UV lines such as Ly α and

O VI $\lambda\lambda$ 1032, 1038. Because most UV spectrometers rely on an entrance slit to separate spatial from spectral information, however, it is unlikely that a spectrograph will be pointed at exactly the right place at the right time. A raster scan of the spectrograph slit can in principle give adequate spatial and spectral coverage, but in practice the raster cadence for the SOHO instruments was on the order of half an hour.

Here we address the thermal conduction problem by observing photons from the flare that are scattered off ions in the corona above the flare, following the methods and results presented by Raymond *et al.* (2007). That way, we measure the total flare luminosity during the impulsive phase in O VI and Ly α lines. Ly α is formed at about 20,000 K, and it dominates the luminosity of the upper chromosphere and lower transition region. O VI is formed at about 300,000 K, near the peak of the radiative cooling curve. The O VI doublet accounts for about 1/8 of the emission at that temperature for solar photospheric abundances, or about 1/16 the total emission between 10^5 and 10^6 K for an emission measure slope like that seen in the quiet Sun or active regions (e.g., Raymond & Doyle 1981).

Figure 1 shows the UVCS observation for the flare of 4 November, 2003, which saturated the GOES detectors, but was at least class X-17. The panel shows the brightness of the O VI λ 1032 line as a function of spatial position along the slit (horizontal direction covering position angles between 303 and 230 degrees from solar North) and time (vertical). The brightening that appears at 19:42 UT (along with a somewhat fainter brightening at 19:33 UT) results from O VI photons scattered from O VI photons in the corona. Immediately after the brightening, the O VI emission fades. This comes about because the CME reaches the position of the UVCS slit, which was placed at $1.63 R_{\odot}$ during this set of observations, and blows the pre-CME corona away.

We know that the O VI brightening results from scattered flare photons for several reasons. First, the emission above the pre-CME background shows a 4:1 intensity

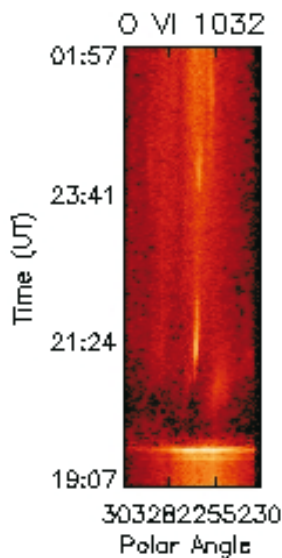


Figure 1. Brightness of the O VI λ 1032 line as a function of time (vertical axis) and position along the UVCS slit.

Table 1. November 4, 2003 energy budget (10^{26} erg s^{-1}).

Event	T_{start}	L_{TR}	L_{therm}	dE/dt
November 4, 2003	19:31:12	2.7	0.7	32
	19:33:22	18.5	7.7	155
	19:35:32	12.2	15.6	-6

ratio between the $\lambda 1032$ and $\lambda 1038$ members of the doublet. This is the value for scattered disk radiation, as opposed to a 2:1 ratio for collisional excitation. Second, the emission appears simultaneously all along the slit, while anything related to CME plasma happens first at the center of the slit and spreads along the slit over the course of ~ 5 minutes. Third, the O VI emission peaks simultaneously with the RHESSI hard X-ray emission. Fourth, the O VI line profile widths and centroids do not change from their pre-CME values.

Several steps are required to derive the luminosity from gas at transition region temperatures. We determine the column density along the line of sight for each pixel along the UVCS slit from the pre-CME intensities of the O VI lines, the scattering cross section and the intensity of O VI emission from the disk (Raymond *et al.* 2007). Then from the column density, the added flux during the flare, and the scattering cross section we compute the luminosity in O VI photons. Finally, we use model calculations of the ratio of O VI luminosity to total transition region luminosity to find L_{TR} . There are a few interesting technical details, most notably the effects of a Doppler shift of the flare emission. Doppler shifts of 20 to 100 km s^{-1} are reported in flares (e.g., Czaykowska *et al.* 1999; Milligan *et al.* 2006). This shifts the flare photons partly away from the absorption profile of the scattering ions in the corona. The effects of the Doppler shift can be determined by comparing the scattered intensity at different places along the UVCS slit, since only the component of velocity along the direction between the flare and the scattering plasma affects the scattering. Among the flares analyzed so far, the Doppler shift ranges up to 90 km s^{-1} .

The overall result of this analysis is that the Ly α and transition region luminosities are comparable. They are on the order of 10% of the rate of increase of the thermal energy of the X-ray emitting plasma if the filling factor of the hot gas is near 1, but they could be comparable if the filling factor is on the order of 0.01.

Table 1 shows the power in different terms in the energy budget for the November 4, 2003 flare in two-minute intervals corresponding to the UVCS exposures. L_{TR} is the transition region luminosity derived from the UVCS observation, L_{therm} is the luminosity of the X-ray emitting thermal plasma, and dE/dt is the rate of change of the thermal energy of the X-ray emitting plasma assuming a filling factor f of 1.0 (Raymond *et al.* 2007). The table shows that the transition region luminosity exceeds the X-ray luminosity for a few minutes during the impulsive phase, but that the X-ray luminosity comes to dominate as cool material is evaporated into the corona.

3. Post-ejection heating

The mass and kinetic energy of CME plasma can be determined from a series of white light coronagraph images (Subramanian & Vourlidas 2007), but the thermal energy is more difficult to determine. UV spectra provide upper limits to the proton and ion

temperatures through the measured line widths, and they provide electron temperatures because of the temperature dependence of the excitation rates of the lines. Moreover, the ionization state of the plasma freezes in, often before the plasma reaches the UVCS slit, so that a UV spectrum gives information about the thermal history of the plasma.

In general, the plasma that shows up brightly in UVCS spectra is relatively cool, typically 50,000 to 500,000 K. That means that its thermal energy is relatively low, $\sim 2 \times 10^{13}$ erg/g, compared to the kinetic energy of 5×10^{15} erg/g for a 1000 km s⁻¹ CME. However, the gas observed by UVCS has expanded by many orders of magnitude by the time it reaches the UVCS slit, and adiabatic cooling would make it much cooler than the observed temperature range if the gas were not heated long after it is ejected from the solar surface. By the time it reaches 1 AU, the temperature is still on the order of 10^5 K, so considerable ongoing heating is required to maintain the temperature.

There are few theories available for the heating of CMEs after the eruption, or for that matter for heating of the plasma during the eruption itself. UVCS is most sensitive to dense, relatively cool material that emits very strongly in ions such as C III, which are completely absent at coronal temperatures. Therefore, ejected prominence material that has not been too strongly heated is the easiest to detect. However, hotter gas is observed by means of O VI, Si XII (2×10^6 K) and [Fe XVIII] ($5\text{--}6 \times 10^6$ K). The last of these represents plasma heated by reconnection during the flare itself, while the O VI and Si XII could be ejected active region material.

One plausible source of heat is the CME-driven shock wave (Raymond *et al.* 2000; Mancuso *et al.* 2002), but that ultimately derives from the CME kinetic energy, and it cannot reach the cool components considered here, so we will not consider it for the energy budget. Another is thermal conduction from hotter coronal material. This may be important for heating electrons at solar wind distances beyond 0.1 AU, since the CME plasma is more or less like relatively fast solar wind at that point. It has more difficulty explaining heating in plasma below 10^5 K, though, because of the strong temperature dependence of the thermal conductivity. Another possibility is wave heating similar to that that heats streamers and drives the quiescent solar wind.

The most interesting possibility was proposed by Kumar & Rust (1996), who suggested that conservation of magnetic helicity in an expanding CME implies the dissipation of magnetic energy. They found that expansion of a self-similar magnetic flux rope transforms comparable amounts of magnetic energy into kinetic energy and plasma heating. They did not really identify the heating mechanism, but they mentioned a turbulent cascade as a likely candidate. More recently, Liu *et al.* (2006) determined the heating rates for interplanetary CMEs at distances between 0.3 AU and 20 AU. They found that heating of protons and alpha particles is consistent with the dissipation of turbulence, and they showed that temperature anisotropies do not drive the turbulence in the inner heliosphere, but they were not able to pin down the source of turbulent energy.

Heating rates have been determined with UVCS in a few cases (Akmal *et al.* 2001; Ciaravella *et al.* 2001; Lee *et al.* 2007). The method is to start with the density either from a density sensitive line ratio such as the ratio of the [O V] forbidden line at 1213.8 Å to the O V] intercombination line at 1218.4 Å, or else from the electron column density from LASCO divided by the line of sight depth from a 3D reconstruction. The temperature and ionization state of the plasma are constrained by the intensities of emission lines such as Ly α , C III and O VI. A large grid of models with different

Table 2. CME energy budgets (10^{13} erg/gm).

	C III ^a	O V ^a	O VI ^a	AH&H ^b	K&R ^b
Kinetic	180	180	180	160	160
Gravitational	78	78	78	56	56
Ionization	1.9	2.1	2.1	2.1	2.1
Thermal	1–3	2–5	3–10	3–4	3.4
Total heat	10–50	50–200	10–500	920–1400	570–690

^aApril 23, 1999 CME.^bDecember 13, 2001 CME.

initial temperatures and densities and with different parameterized heating rates is computed, and for a CME feature with good enough observations, nearly all those models can be eliminated. Note that any heating of the plasma during the very early stages of the eruption is included in the initial temperature specified. Such heating tends to strongly affect the ionization state of the plasma, but it is rapidly lost to adiabatic expansion.

The integrated heating of the models that match the observations tends to lie in a range of about an order of magnitude for the Akmal *et al.* (2001) and Ciaravella *et al.* (2001) analyses or somewhat less for the cases analyzed by Lee *et al.* (2007). The total heat that must be added to the plasma after ejection is comparable to or larger than the kinetic energy as shown in Table 2. The results for the April 23, 1999 and December 13, 2001 events are taken from Akmal *et al.* (2001) and Lee *et al.* (2007), respectively. The first three columns show results for 3 different knots of plasma bright in C III, O V and O VI, respectively, for the April 1999 event at $3.5 R_{\odot}$ (Akmal *et al.* 2001). The last two columns show results for one knot for the December 2001 event at $2.9 R_{\odot}$ for heating rates given by the functional forms of Allen *et al.* (1998) and of Kumar & Rust (1996) indicated by AH&H and by K&R, respectively (Lee *et al.* 2007).

Overall, we find that the heat input to CME plasma after ejection from the Sun is comparable to the kinetic energy in all but the coolest knots, and larger than the kinetic energy in some cases. This energy is important for a complete physical understanding of CMEs, but we must still narrow down the possible sources of that energy.

Acknowledgement

This work was supported by NASA grants NAG5-12827 and NNG06G188G to the Smithsonian Astrophysical Observatory.

References

- Akmal, A., Raymond, J. C., Vourlidas, A., Thompson, B., Ciaravella, A., Ko, Y.-K. Uzzo, M., Wu, R. 2001, *ApJ*, **557**, 922.
 Allen, L. A., Habbal, S. R., Hu, Y. Q. 1998, *JGR*, **103**, 6551.
 Aschwanden, M. J., Aschwanden, P. D. 2006, preprint.
 Ciaravella, A., Raymond, J. C., Reale, F., Strachan, L., Peres, G. 2001, *ApJ*, **557**, 351.
 Czaykowska, A., De Pontieu, B., Alexander, D., Rank, G. 1999, *ApJL*, **521**, L75.
 Emslie, A. G., Dennis, B. R., Holman, G. D., Hudson, H. S. 2005, *JGR*, **110**, A11103.
 Holman, G. D., Sui, L., Schwartz, R. A., Emslie, A. G. 2003, *ApJ*, **595**, L97.

- Innes, D. E., Curdt, W., Schwenn, R., Solanki, S., Stenborg, G., McKenzie, D. E. 2001, *ApJL*, **549**, L249.
- Kohl, J. L., Noci, G., Cranmer, S. R., Raymond, J. C. 2006, *A&A Rev.*, **13**, 31.
- Kumar, A., Rust, D. M. 1996, *JGR*, **101**, 15,667.
- Lee, J.-Y., Raymond, J. C., Ko, Y.-K., Kim, K.-S. 2007, in preparation.
- Liu, Y., Richardson, J. D., Belcher, J. W., Kaper, J. C. 2006, *JGR*, **111**, A01102.
- Mancuso, S., Raymond, J. C., Kohl, J., Ko, Y.-K., Uzzo, M., Wu, R. 2002, *A&A*, **383**, 267.
- Milligan, R. O., Gallagher, P. T., Mathoudiakis, M., Bloomfield, D. S., Keenan, F. P., Schwartz, R. A. 2006, *ApJL*, **638**, L117.
- Pike, C. D., Mason, H. E. 2002, *Solar Phys.*, **206**, 359.
- Raymond, J. C., Doyle, J. G. 1981, *ApJ*, **246**, 686.
- Raymond, J. C., Thompson, B. J., St. Cyr, O. C. *et al.* 2000, *GRL*, **27**, 1439.
- Raymond, J. C., Holman, G., Ciaravella, A., Panasyuk, A., Ko, Y.-K., Kohl, J. L. 2007, *ApJ*, **659**, 750.
- Schwenn, R. *et al.* 2006, *SSRV*, **123**, 127.
- Subramanian, P., Vourlidas, A. 2007, astro-ph/0701160.